Available online at www.sciencedirect.com
ScienceDirect
Food Chemistry 103 (2007) 994–1002
Food Chemistry
www.elsevier.com/locate/foodchem

Effects of acid modification on physical properties of konjac glucomannan (KGM) films

L.H. Cheng [a], A. Abd Karim [a,*], C.C. Seow [b]

[a] Food Technology Division, School of Industrial Technology, Universiti Sains Malaysia, 11800 Penang, Malaysia
[b] Food Technology Consultant, 209 Solok Pemancar, 11700 Gelugor, Penang, Malaysia

Accepted 15 September 2006

Abstract

Edible films prepared from partially acid-hydrolyzed konjac glucomannan (KGM) were characterised with respect to the influence of altered chain length and molecular weight distribution on water sorptive capacity (WSC), water vapour permeability (WVP), thermal, and tensile properties. Acid treatment produced films with higher WSC and WVP, and lower melting enthalpy than that of an untreated one. These effects were attributed to an increase in the number of shorter chains, which contributed to more active sites for moisture sorption but disfavoured the formation of junction zones. The elastic modulus (EM) and tensile strength (TS) increased initially with decreasing molecular weight and increasing polydispersity, and then decreased with further reduction in molecular weight. Conversely, tensile elongation (TE) exhibited the opposite trend.

Keywords: Konjac glucomannan; Edible films; Acid modification; Molecular weight; Size-exclusion chromatography; Mechanical properties

1. Introduction

Research and development of edible films are challenging because agromaterials have diverse characteristics and cause effects vastly differ from one another. Different film ingredients and formulations will produce films with different characteristics. This has driven intensive research to identify and modify the existing film ingredients and formulations in order to meet the increasing demand for edible films for specific applications of premium products. Blending, plasticization and incorporation of hydrophobic materials are the common techniques for modifying film properties. One example was demonstrated by Ofori-Kwakye and Fell (2001), in which protein/chitosan/hydroxypropylmethylcellulose (HPMC) films show potential for controlled biphasic drug release characteristics, by manipulating the HPMC compositions. It was reported that minimum permeability was obtained at pH 3 and at an HPMC level of 5% where pectin and chitosan interact to form a polyelectrolyte complex that limits drug diffusion of the films. The film permeabilities increased on exposure to pectinolytic enzymes, which confirms the potential of pectin/chitosan/HPMC films for controlled delivery, with an initial slow phase, followed by a faster phase under conditions prevailing in the colon.

Acid hydrolysis is a potentially useful method for altering film properties because hydrolyzed products have different molecular masses and physicochemical properties. According to Chanda and Roy (1998), molecular weight distribution determines, to a certain extent, the general behaviour of a polymer. Examples of improved performance of biopolymers achieved through acid hydrolysis are given below:

(a) thin boiling starch, an acid-modified starch, has found its way into the candy industries where it allows the use of highly concentrated fluid paste to form firm gels upon cooling and aging (Rohwer & Klem, 1984),

* Corresponding author. Tel.: +60 4 6532221; fax: +60 4 6573678.
E-mail address: akarim@usm.my (A. Abd Karim).

0308-8146/$ - see front matter © 2006 Elsevier Ltd. All rights reserved.
doi:10.1016/j.foodchem.2006.09.052

(b) acid-hydrolyzed whey protein isolate was reported to be able to reduce the allergenicity of milk protein (Nielsen, 1997),
(c) acid-hydrolyzed starch tailing fractions have been reported to be used as bulking agents to replace sucrose in cookies, resulting in very slight cookie spread (Krishnarau & Hoseney, 1994).

To the best of our knowledge, information on edible films derived from acid-modified biopolymers is limited to the work on whey protein isolate (WPI) (Sothornvit & Krochta, 2000a, 2000b), and potato starch (Shamekh, Myllarinen, Poutanen, & Forssell, 2002). Acid-hydrolyzed WPI films possessed mechanical properties similar to those of unhydrolyzed WPI films but exhibited enhanced solubility and gas barrier properties. It was also reported that a reduction in WPI molecular weight was a better approach for improving film flexibility than was addition of plasticizers, such as glycerol. For hydrolyzed potato starch, a solution with as much as 10–20% solids content could be used to form good quality films. In addition, the dissolution procedure could be carried out at a relatively lower temperature (120 °C) for hydrolyzed potato starch compared to native starch (160 °C).

Knowing the significant effects brought about by acid modification of biopolymers, the present work was undertaken in an attempt to study, in greater detail, the properties of edible films derived from acid-modified KGM.

2. Materials and methods

2.1. Materials

Purified KGM (PROPOL A) was obtained from Shimizu Chemical Corporation, Japan. Concentrated hydrochloric (HCl) acid (36% v/v) and ethyl alcohol (EtOH, 99.7% v/v) from R&M Chemicals were used in this study.

2.2. Acid modification

KGM (35 g) was suspended in 250 ml of absolute alcohol, in which a controlled amount of concentrated HCl (10, 20, 30, 50, or 70 ml) was pre-added. Absolute alcohol was used to prevent swelling of KGM particles and ensure low viscosity of the suspension. The suspension, in a screw-capped Erlenmayer flask, was magnetically stirred for 2 h at room temperature, filtered through Whatman No. 1 filter paper and washed with 70% EtOH until the washings became neutral to litmus. The samples were then left in a fume hood before being subjected to vacuum-drying at 30 °C for 16 h. The native and acid-hydrolyzed KGM were kept in separate airtight containers for at least two days. The moisture contents were subsequently determined by oven drying at 105 °C for 24 h. The samples were coded as KGM-0HCL for native KGM, and as KGM-10HCL, KGM-20HCL, KGM-30HCL, KGM-50HCL and KGM-70HCL, for samples treated with 10, 20, 30, 50, and 70 ml HCl, respectively.

Analysis of variance (ANOVA) and general linear model were carried out on the experimental data obtained, using Minitab For Windows, Release 10.1 (Minitab Inc., State College, PA).

2.3. Scanning electron microscopy

KGM particles (native and acid-hydrolyzed) were mounted on a specimen stub and coated with 100–200 Å thickness of gold in a Polaron SC515 scanning electron microscopy (SEM) coating system. The specimen was scanned using a Leica Cambridge S-360 electron microscope. Images were recorded on Kodak Plus-X pan films.

2.4. Distribution of chain lengths

Sample preparation for HPLC analysis was done by solubilizing 0.1 g (dry weight) of KGM in 100 ml of distilled, deionized water. The solution was then stirred for 4 h and filtered through 0.45 μm membrane filter before being subjected to HPLC analysis. The HPSEC method was adapted from Cui and Oates (1999) with some modifications (described below).

A Waters Associates (Milford, MA, USA) 2690 series liquid chromatography system and a model 2410 refractive index detector were used. The refractive index detector sensitivity (8) and scale factor (60) were fixed for all determinations. Columns were connected in the following order: Ultrahydrogel guard column, followed by Ultrahydrogel linear (7.5 mm × 300 mm) and one Ultrahydrogel 250 (7.5 mm × 300 mm). The Ultrahydrogel column was packed with cross-linked methacrylate gel. Ultrahydrogel linear has a blend pore size with an exclusion limit of 7×10^6. Ultrahydrogel 250 has an exclusion limit of 8×10^4. The columns and refractometer were maintained at 60 and 35 °C, respectively, and calibrated by using pullulan standards (P-800, P-400, P-200, P-100, P-50, P-20, P-10, P-5). The mobile phase was distilled, deionized water at a flow rate of 1.0 ml/min.

2.5. Intrinsic viscosity [η] measurement

To determine intrinsic viscosity [η] of each KGM sample (native or acid-hydrolyzed), a solution of 0.05 g/dl in distilled water was prepared and centrifuged at 1700*g* for 15 min. After holding for 1 h, the viscosity of the supernatant was then measured with a dilution Ubbehlode-type viscometer (Cannon Instrument, State College, PA), which was immersed in a constant temperature bath pre-set at 10, 20, 30 or 40 °C. The flow time of the solution through the capillary tube of the Ubbehlode viscometer was measured.

The [η] was determined through the measurement of the specific polymer viscosities, defined as

$$\eta_{sp} = \frac{t - t_0}{t_0}$$

where η_{sp} is the specific polymer viscosity, t and t_0 are the flow time of the polymer solutions and the pure solvent, respectively. The $[\eta]$ was then determined as the limit of the ratio between the specific viscosity and the polymer solution concentration (c) when the polymer concentration (g/dl) approaches zero.

$$[\eta] = \lim_{c \to 0} \frac{n_{sp}}{c}$$

2.6. Films preparation and characterization

2.6.1. Preparation

To produce KGM films (native and acid-hydrolyzed), 7 g (dry basis) of KGM sample were added to 1 l distilled water and blended for 15 min in a National® home blender (Model MX-595 N). The mixture was left to stand for 1 h at 30 °C, after which 90 g portions were poured and spread onto a level, square Perspex mould with a 16 × 16 cm film-forming area. The solutions were then left to dry at room temperature for ~20 h. Films formed were peeled off and kept in zippered HDPE plastic bags.

2.6.2. Wide-angle X-ray diffraction (WAXD)

Films were conditioned at 30 °C and 69% RH (over a saturated strontium chloride solution) for 7 days prior to subjecting to WAXD analysis. Conditioned samples were scanned using a D5000 SIEMENS X-ray powder diffractometer equipped with a CuK_α target at 40 kV and 20 mA. WAXD patterns at diffraction angles ranging from $2\theta = 5°$ to 50° were recorded using a scintillation detector.

2.6.3. Sorption isotherm measurement

Sorption isotherms of the films studied were determined at 30 °C according to the procedure described by Spiess and Wolf (1983). Films were cut into small pieces and pre-dried over phosphorus pentoxide (P_2O_5) under vacuum at room temperature for a week to obtain "zero" water content. About 200 mg dried films were weighed into pre-weighed weighing bottles. The dried samples, in quadruplicate, were equilibrated in Kilner jars containing different saturated salt solutions of known relative vapour pressure (RVP) at 30 °C (Greenspan, 1977). The saturated salt solutions used were lithium chloride, potassium acetate, magnesium chloride, potassium carbonate, sodium bromide, strontium chloride, sodium chloride, and potassium chloride, with RVP of 0.11, 0.22, 0.32, 0.43, 0.56, 0.69, 0.75 and 0.84, respectively. Samples weights were monitored daily. "Equilibrium" was assumed to have been achieved when the change in weight did not exceed 0.1% for three consecutive weighings. Moisture content (dry basis) was calculated from the weight gained.

2.6.4. Water vapour permeability (WVP) determination

WVP tests were conducted according to ASTM (1981a) Method E96-80. The film sample was sealed as a patch onto a glass permeation cell containing silica gel (RVP = 0) with a 1.5 cm-deep headspace. The cell was incubated in a desiccator maintained at 30 °C and RVP = 0.22 by using a saturated salt solution of potassium acetate. The dull side of the cast film was facing the higher RVP compartment, and water vapour transport was determined from the weight gain of the cell. The cell weight was monitored daily over a 6-day period. Changes in weight of the cell were plotted as a function of time. The water vapour transmission rate (WVTR) was calculated from the slope of the constant rate of weight gain ($R^2 \geqslant 0.99$) divided by the test area. WVTR ($kg\,s^{-1}\,m^{-2}$) for each film type was determined with two individually prepared films as the replicated experimental units and three sub-samples tested from each film. WVP ($kg\,Pa^{-1}\,s^{-1}\,m^{-1}$) was calculated as $WVP = [WVTR/S(R_1 - R_2)] \times d$, where S = saturation vapour pressure (Pa) of water at test temperature, R_1 = RVP in the desiccator, R_2 = RVP in the permeation cell, and d = film thickness (m). Film thickness was measured using a micrometer (Mitutoyo, Japan).

2.6.5. Differential scanning calorimetry

Differential scanning calorimetry (DSC) was performed using a DuPont 2910 differential scanning calorimeter (E.I. DuPont de Nemours & Co., Inc., Wilmington, Del., USA). Films were cut into small pieces. The cut sample pieces were equilibrated under vacuum for approximately 7 days at a relative humidity of 56% over a saturated salt solution of sodium bromide at 30 °C (Greenspan, 1977). Samples (of 8–10 mg each) were hermetically sealed in aluminium sample pans, using an inverted lid configuration. Samples were heated from room temperature to 270 °C at a heating rate of 20 °C min^{-1} and an oxygen-free nitrogen flow rate of 30 ml min^{-1}. The transition temperatures (onset, T_o; and peak, $T_{p)}$ and enthalpy of melting (ΔH) for each film type were determined with two individually prepared films as the replicated experimental units and two sub-samples.

2.6.6. Tensile measurement

Tensile tests were performed according to ASTM (1981b) Method D882-80a. Film strips of 14.0 × 1.5 cm dimension were stretched at 0.2 mm s^{-1} using a TA.XT2™ Texture Analyzer (Stable Micro System, Surrey, UK). Films strips were conditioned at RVP = 0.22, 0.43, 0.69 and 0.84 under vacuum over saturated salt solutions at 30 °C for at least 4 days. The reported mean value for each film type was determined with three individually prepared films as the replicated experimental units and four sub-samples tested for each film. Tensile strength (TS, Pa) was calculated by dividing the maximum load by the original cross-sectional area of the specimen. Elastic modulus (EM, Pa) was calculated from the slope of the initial linear portion of the stress–strain curve. Tensile elongation or strain-at-break (TE, %) was calculated by dividing the

elongation at the moment of rupture of the specimen by the initial gauge length (10.0 cm) of the specimen and multiplying by 100.

3. Results and discussion

3.1. Morphology

Morphological properties of native and acid-hydrolyzed KGM granules were observed by scanning electron microscopy. Fig. 1a shows an overview of native KGM granules at low magnification. KGM granules were found to possess irregular shapes. When the surface of a particular KGM granule was focussed and magnified at a higher level (Fig. 1b), scale-like surfaces were clearly shown. Similar scale-like surfaces, which were more obvious when a higher degree of KGM purification was achieved, were similarly observed by Takigami (2000). Nevertheless, smooth surfaces were occasionally observed (Fig. 1a) – these appeared to be fracture surfaces, probably arising from mechanical damage of the KGM granules during processing. Fig. 1c was obtained from an acid-hydrolyzed sample and the micrograph taken was focussed on a fractured surface with signs of acid erosion. It is noteworthy that the highly organized scale-like surfaces remained practically unchanged, irrespective of the amount of acid added. However, deep round "craters" and surface erosion, indicative of acid attack, were clearly evident on the smooth surfaces of fractured granules (Fig. 1c). It is suggested that the outer surfaces of a KGM granule are resistant to acid hydrolysis, probably due to the presence of a protecting fibrous membrane (Takigami, Takiguchi, & Philips, 1997). Fig. 1d and e are micrographs for KGM-50HCL and KGM-70HCL, respectively. Micrographs of KGM at other acid concentrations are not shown because of limited acid erosion. More severe acid erosion appeared to have occurred in KGM-70HCL than in KGM-50HCL, as indicated by the number, size and depth of the "craters" observed.

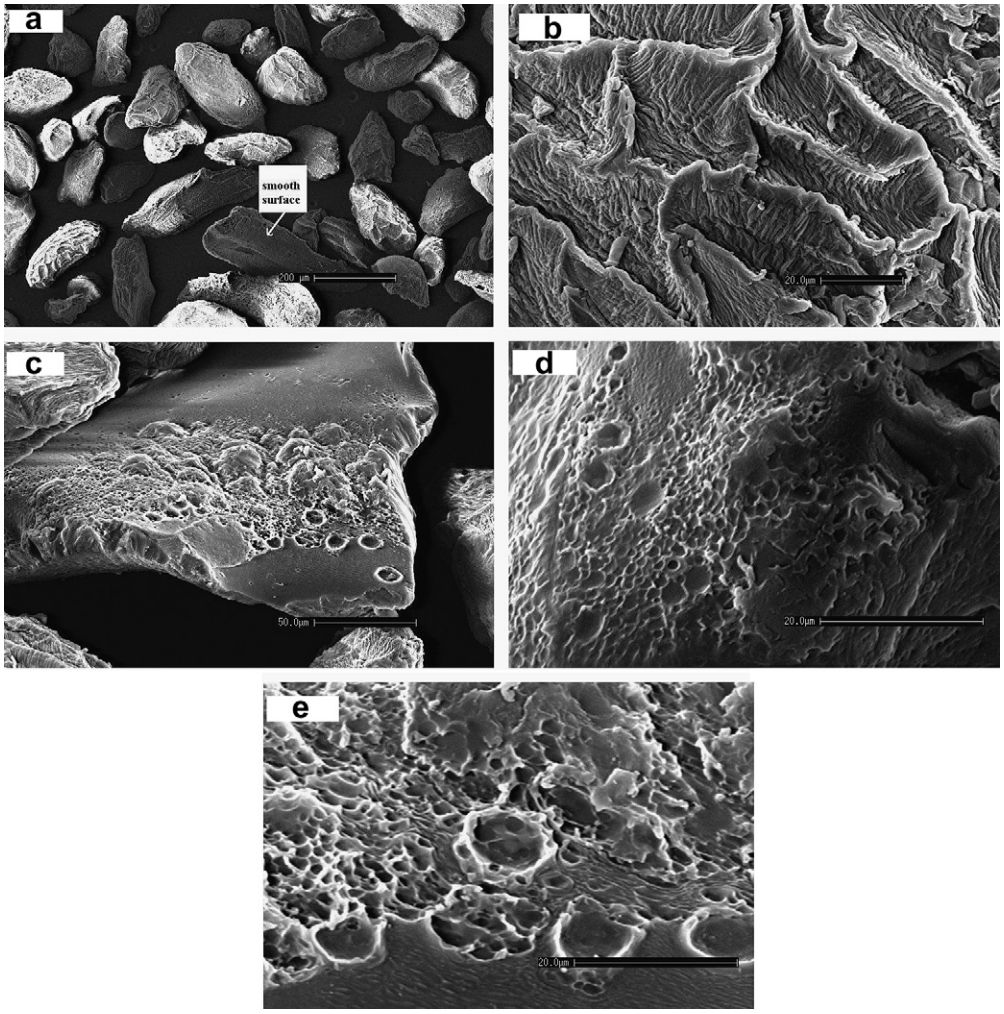

Fig. 1. Scanning electron micrographs of KGM granules. (a) Overall view of native KGM granules, (b) scale-like surface of a KGM granule, (c) acid attacks on a smooth surface of a fractured granule, (d) surface morphology of a particular KGM-50HCl sample, (e) surface morphology of a particular KGM-70HCL sample.

3.2. Molecular mass properties

The distribution of molecular size and weight-average molecular weight of KGM samples were studied by size exclusion chromatography (SEC) and the molecular mass properties are shown in Table 1. Results displayed for each sample show the SEC data (apparent number average molecular weight, M_n, apparent weight-average molecular weight, M_w, and apparent polydispersity, I), calculated from SEC retention time based on pullulan calibration.

From Table 1, the weight-average molecular weight value for native KGM is 3.78×10^6 which is slightly higher than the value (2.00×10^6) reported in the Glucomannan Propol® catalogue provided by Shimizu Chemical Corporation. This discrepancy may be attributed to the different methodologies applied and the molecular weights obtained in this study are regarded as equivalent pullulan molecular weights. Elution time and M_w are two useful indications of efficiency of acid treatment on a polymer. As shown in Table 1, the elution time became progressively longer and M_w progressively lower with increasing amounts of acid added to the suspension. The trend observed for M_w was also evident for M_n, except for KGM-50HCL, which gave rise to two distinct fractions. Polydispersity index (I) provides a simple definition of molecular weight distribution. The higher the value of I, the greater is the spread of the molecular weight distribution of the polymer. For a monodisperse system, $I = 1$ (Chanda & Roy, 1998). Our results showed no regular pattern in I as depolymerization proceeded with increasing HCl concentration. Overall, KGM-30HCL possessed a molecular weight lower than the control and the highest value of I (3.86). It is suggested that KGM-30HCL possessed relatively more lower molecular weight fractions than did the other samples.

3.3. Intrinsic viscosity [η]

Viscosity measurements provide the most convenient and accurate way to determine the relative sizes of molecules. The viscometric parameter of importance is the limiting viscosity number or intrinsic viscosity, [η], which would decrease considerably with molecular degradation. The quantity [η] of a polymer solution is a measure of the capacity of the polymer molecule to enhance viscosity that, in turn, depends on the size and the shape of the polymer molecule (Kurata & Tsunashima, 1989). In other words, a higher value of [η] indicates a more extended chain in solution, which increases the chances of inter-molecular entanglements. Therefore, it is generally accepted that within a given series of polymer homologues, [η] increases with molecular weight (Kurata & Tsunashima, 1989).

Fig. 2 shows the variations of [η] as a function of $1/T$. It is obvious that [η] decreased linearly with a progressive decrease in $1/T$ ($P < 0.01$). This is in good agreement with the work of Chen and Tsaih (1998) who studied the effect of temperature on the intrinsic viscosity and conformation of chitosans in dilute HCl solution. Chen and Tsaih (1998) reported that increasing the solution temperature usually resulted in a rapid decrease in the ratio of radius of gyration and average molecular weight – hence chain compactness increased correspondingly, thereby resulting in a decrease in the intrinsic viscosity. In addition, increasing temperature may result in a decrease in hydrogen-bonded hydration water, thus causing a decrease in intrinsic viscosity.

Table 1
Molecular mass properties of native and acid-treated KGM samples

Sample	Number of distinct fraction	Elution time (min)	$M_n \times 10^{-5}$ [a]	$M_w \times 10^{-5}$ [b]	I [c]
KGM-0HCL	1	11.498	11.3	37.8	3.35
KGM-10HCL	1	11.703	9.0	31.1	3.46
KGM-20HCL	1	11.821	6.6	24.4	3.70
KGM-30HCL	1	11.874	5.3	20.6	3.86
KGM-50HCL	2	12.057	9.5	17.4	1.83
		12.967	1.3	1.8	1.38
KGM-70HCL	1	13.195	1.4	4.1	2.93

[a] M_n = apparent number average molecular weight.
[b] M_w = apparent weight-average molecular weight.
[c] I = apparent polydispersity.

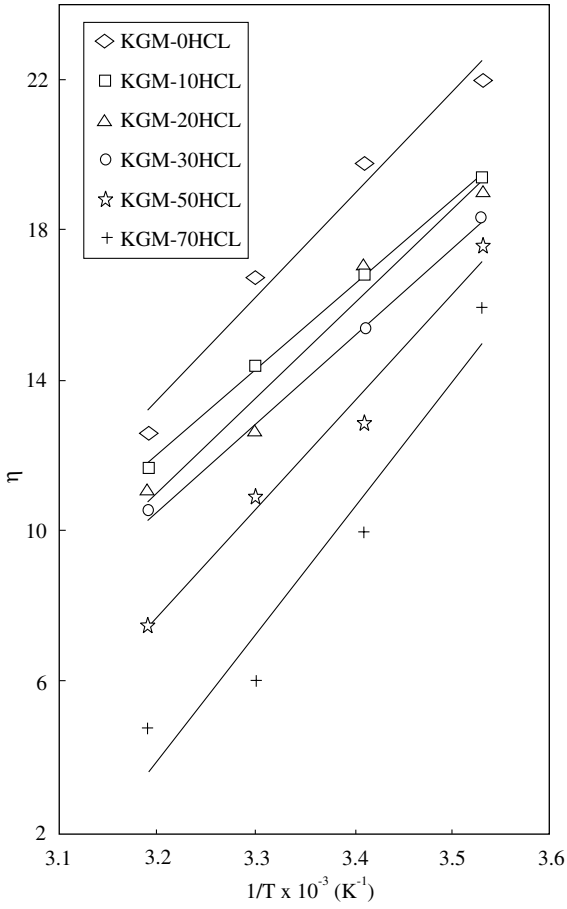

Fig. 2. Plot of intrinsic viscosity [η] versus inverse of absolute temperature ($1/T$, K^{-1}) of native and acid-hydrolyzed KGM samples.

By checking on the values of the slope of $d[\eta]/d(1/T)$, it is obvious that the partial hydrolysis brought about a significant ($P < 0.01$) change in molecular properties of KGM chains. KGM-50HCL and KGM-70HCL showed a more abrupt decrease in $[\eta]$ as temperature increased. This could be attributed to the reduced chain flexibility of shorter molecular chains (Chen & Tsaih, 1998). This assumption is substantiated by the results obtained from the present SEC study where KGM-0HCL, KGM-10HCL, KGM-20HCL and KGM-30HCL were found to possess molecular weights of the same order, that is 37.8×10^5, 31.1×10^5, 24.4×10^5 and 20.6×10^5, respectively. On the other hand, molecular weights of KGM-50HCL and KGM-70HCL were reduced by one order of magnitude, as shown in Table 1.

3.4. Film characterization

3.4.1. Preparation

The films obtained were transparent, flexible and easily peeled from the casting perspex board. It should be noted that the acid modification was limited to the range selected, to facilitate handling and casting of the film-forming solution. Too high a modification level would result in excessively low solution viscosity, thus making it impossible to cast the film.

3.4.2. Crystallinity

The X-ray diffraction patterns of the native and acid-hydrolyzed KGM samples are shown in Fig. 3. Looking at the diffraction pattern, only weak and broad prominent peaks were observed. Unfortunately, no obvious trend could be observed in terms of peak intensity or locality as a function of the level of acid modification. All samples studied exhibited hump-like diffuse peaks within the 2θ range of 13–22°. Generally, this would suggest that pure KGM films are highly amorphous with low crystallinity, despite the effect of molecular size and molecular weight. Lack of stereoregularity along the backbone of KGM molecules could account for the low crystallinity characteristics. This is because KGM is a copolymer of mannose and glucose with a random and occasional occurrence of acetyl groups at the saccharide units along the molecule.

3.4.3. Sorption isotherm

Fig. 4 shows the moisture sorption isotherms of the films studied. Statistical analysis of the sorption data obtained showed that acid hydrolysis of the KGM chains has significant ($P < 0.01$) effects on the sorption isotherms of the films obtained. The results obtained clearly show that water binding capacity of the films increased progressively with increasing hydrolysis (i.e. decreasing molecular weight). It is suggested that lower molecular weight chains would possess more active sites for water sorption than would higher molecular weight chains on a per unit mass basis. This is because, when a polymer chain is hydrolyzed, more chain ends with polar (–OH) groups are produced.

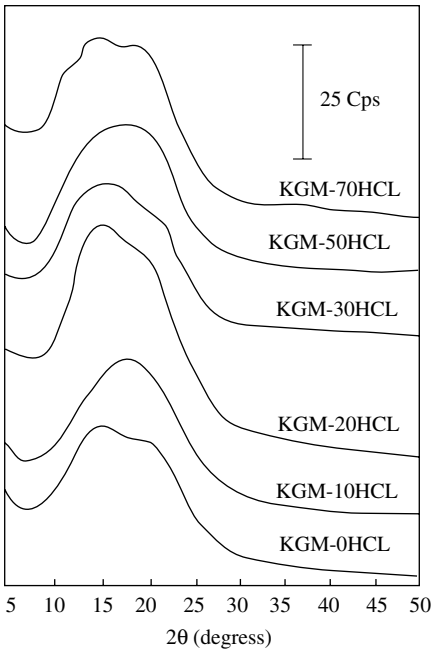

Fig. 3. The wide-angle X-ray diffraction patterns of native and acid-hydrolyzed KGM films.

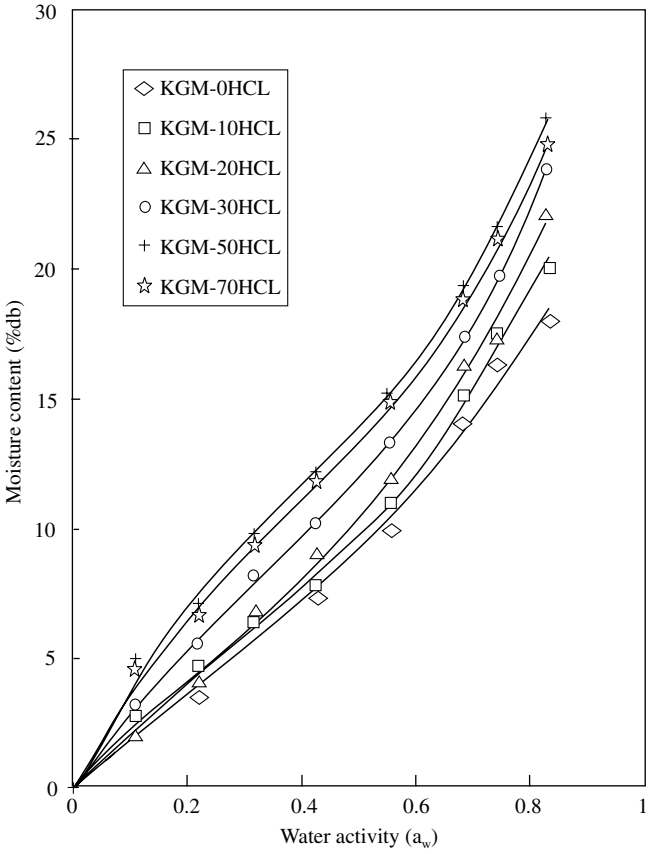

Fig. 4. Moisture sorption isotherm of native and acid-hydrolyzed KGM films at 30 °C. (Typical coefficient of variations (CV) for quadruplicate measurements did not exceed 10%).

3.4.4. Water vapour permeability (WVP)

WVP data of the films studied are given in Table 2. Water vapour transmission through a polymer film basically involves three steps: adsorption of water molecules onto the film surface, diffusion of the water molecules through the film matrix, and discharge of the water molecules from the opposite surface to a low humid environment. Table 2 shows that acid hydrolysis significantly ($P < 0.01$) increased WVP of the films. As suggested by Cheng, Abd Karim, Norziah, and Seow (2002), WVP of a film is believed to be dependent on the number of "available" polar (–OH) groups that the polymer possesses. Since more polar chain ends would have been produced during acid hydrolysis, this would facilitate the adsorption of water molecules onto the external surface of the film. Furthermore, it is believed that the film matrix produced from lower molecular weight KGM chains would swell more easily. This is supported by Yoshimura and Nishinari's (1999) work, which showed that gels prepared from low molecular weight KGM exhibited lower elastic moduli. They attributed this phenomenon to the low tendency of low molecular weight KGM to form junction zones. They suggested that the flexible molecular chains connecting the junction zones would become shorter with decreasing molecular weight. Therefore, water molecules would diffuse more easily through the film matrix formed from lower molecular weight KGM. The WVP results are also consistent with the moisture sorption data.

3.4.5. Thermodynamic properties

Thermodynamic properties of the films studied are also shown in Table 2. In general, enthalpy of melting of crystalline structure within a KGM film appeared to significantly ($P < 0.05$) decrease, progressively, with decreasing molecular weight, except for KGM-30HCL. However, acid hydrolysis over the extent studied appeared to have no significant ($P > 0.05$) effect on the onset and peak temperatures. According to Chen, Tsaih, and Lin (1996), enthalpy of melting can be used as a quantitative index of hydrogen bond formation in the system analyzed. A higher enthalpy indicates the presence of more hydrogen bonds in the system. In the present context, shorter chains would disfavour the formation of junction zones and the number of hydrogen bonds formed within a junction zone would be comparatively lower (Yoshimura & Nishinari, 1999). However, with relatively higher amount of low molecular weight tailings in the sample, as observed in KGM-30HCL, chain alignment was enhanced.

3.4.6. Tensile properties

The effects of molecular weight on film elastic modulus (EM), tensile strength (TS), and tensile elongation (TE) as a function of water activity (a_w) and amount of acid treatment given are shown in Figs. 5–7, respectively.

Figs. 5 and 6 show that EM and TS of the films increased significantly ($P < 0.01$) to a maximum with increased KGM hydrolysis to a level corresponding to 30 ml HCl/250 ml alcohol, after which EM and TS decreased as the extent of hydrolysis was further extended. The opposite trend was observed in the case of *TE*. Such trends were also reported by Grosvenor and Staniforth (1996), and Abd El-Kader, Abdel Hamied, Mansour, El-Lawindy, and El-Tantaway (2002) who studied the effect of molecular weight on the properties of poly(ε-caprolactone) and poly(vinyl alcohol), respectively. To understand

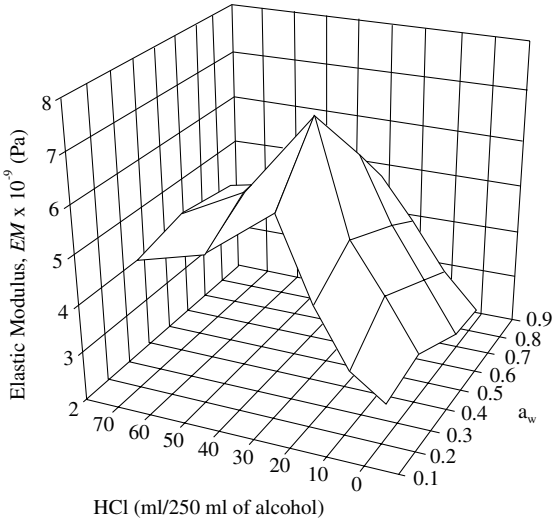

Fig. 5. Elastic moduli of native and acid-hydrolyzed KGM films as a function of a_w.

Table 2
Water vapour permeability and the DSC transition temperatures and melting enthalpy of films prepared from native and acid-hydrolyzed KGM

Films type	WVP × 10^{14} (kg Pa^{-1} s^{-1} m^{-1})[1]	Transition temperature (°C)[2]		Enthalpy[2] ΔH (J g^{-1})
		Onset (T_o)	Peak (T_p)	
KGM-0HCL	1.20 ± 0.07^{e}	110.1 ± 1.9^{a}	136.1 ± 11.3^{a}	275.6 ± 5.0^{a}
KGM-10HCL	1.35 ± 0.07^{de}	107.8 ± 2.5^{a}	126.0 ± 7.1^{a}	259.5 ± 9.9^{ab}
KGM-20HCL	1.41 ± 0.05^{cd}	110.3 ± 1.4^{a}	136.7 ± 7.2^{a}	241.7 ± 4.7^{bc}
KGM-30HCL	1.50 ± 0.05^{bc}	110.9 ± 4.3^{a}	141.1 ± 9.4^{a}	253.9 ± 5.3^{ab}
KGM-50HCL	1.59 ± 0.04^{ab}	108.4 ± 0.3^{a}	126.2 ± 3.0^{a}	230.7 ± 3.8^{c}
KGM-70HCL	1.64 ± 0.04^{a}	116.3 ± 1.9^{a}	152.3 ± 7.3^{a}	219.7 ± 3.5^{c}

Means within a column with the same letter are not significantly different at the 5% probability level.
[1] Mean ± SD ($n = 6$).
[2] Mean ± SD ($n = 4$).

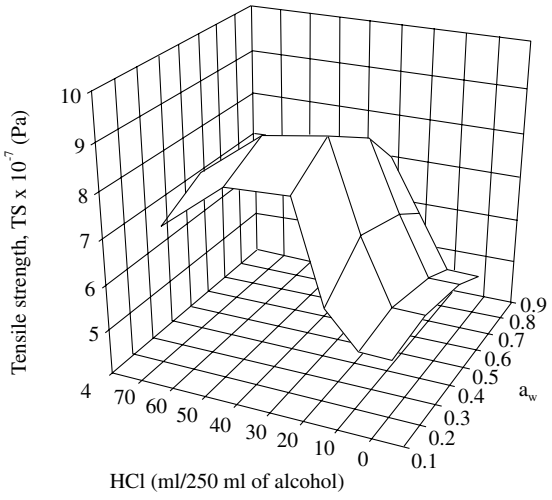

Fig. 6. Tensile strength of native and acid-hydrolyzed KGM films as a function of a_w.

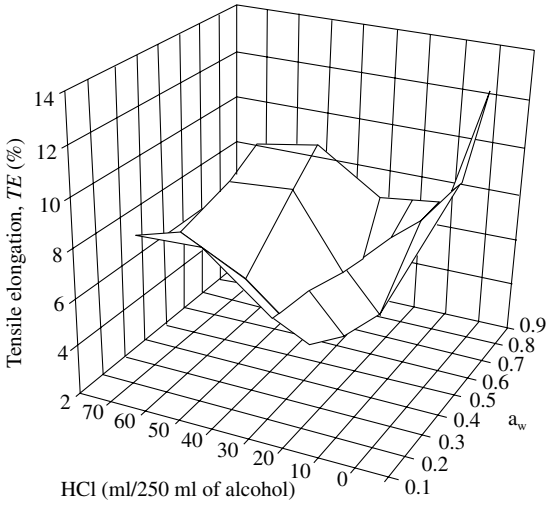

Fig. 7. Tensile elongation of native and acid-hydrolyzed KGM films as a function of a_w.

the phenomenon observed, one has to take into consideration other factors that play a significant role besides chain length, such as chain flexibility and mobility, degree of entanglement, and available segmental motion (Chen et al., 1996; Grosvenor & Staniforth, 1996; Yoshimura & Nishinari, 1999; Zhang et al., 2001). Another factor that should not be forgotten is the possible plasticizing or antiplasticizing effects exerted by the small molecular weight tailings present in each molecular distribution.

Incomplete chain alignment because of extensive entanglements of high molecular weight chains may account for the increase in EM and TS and decrease in TE, as M_w decreased. In addition, low molecular weight tailings could act as a slippage area between longer polymer chains to confer a higher degree of viscous flow in the film-forming solution. This would probably favour chain alignment through greater hydrogen bonding during the day-long drying process. This explanation appears to be consistent with the results of molecular mass analysis, in which polydispersity of the acid-hydrolyzed samples increased in the order: KGM-0HCL < KGM-10HCL < KGM-20HCL < KGM-30HCL. On the other hand, antiplasticization, where free volume between polymer chains in the amorphous phase could be filled or fitted with small molecular weight tailings, could also cause the film matrix to become stiffer and denser, hence giving a higher EM and TS, but a lower TE. However, the actual mechanisms involved cannot be fully elucidated at this time.

On the other hand, a decrease in EM and TS, and increase in TE with reduced M_w may also occur. When compared with higher molecular weight chains, the lower molecular weight chains have little opportunity to form entanglements between chains, owing to stiffer chain lengths. This is because entanglements play an important role in limiting segmental mobility and facilitate chain alignments within entanglements. However, beyond a certain limit, additional entanglements may bring about detrimental effects, as previously described. Therefore, KGM-50HCL and KGM-70HCL have relatively low EM and TS, but high TE as compared to KGM-30HCL.

For each film type studied, EM and TS showed an initial increase, followed by a decrease as the films were humidified, with maximum EM and TS and minimum TE occurring at $0.43a_w$. This appears to be a case of antiplasticization by water at low a_w, a rather common phenomenon in biopolymer films previously reported by many other researchers (Chang, Cheah, & Seow, 2000; Cheng et al., 2002; Gontard, Guilbert, & Cuq, 1993; Kumar, Bhandari, & Bhat, 1991).

4. Conclusions

This study showed that acid modification allows biopolymers to be tailored made to give specific film properties. By controlling degree of acid hydrolysis and molecular weight and molecular weight distribution of the polymers, film water sorptive capacity, water vapour permeability and thermal and tensile properties can be regulated.

Acknowledgements

LHC is grateful to Universiti Sains Malaysia for the award of a fellowship under the Academic Staff Training Scheme. This work was supported by an 8th Malaysia Plan R&D grant under the Intensification of Research in Priority Areas (IRPA) Programme of the Ministry of Science, Technology and Environment, Malaysia.

References

Abd El-Kader, K. A. M., Abdel Hamied, S. F., Mansour, A. B., El-Lawindy, A. M. Y., & El-Tantaway, F. (2002). Effect of the molecular weights on the optical and mechanical properties of poly(vinyl alcohol) films. *Polymer Testing, 21*, 847–850.

ASTM (1981a). Standard test method for water vapor transmission of materials. *Method E96-80*. Philadelphia: American Society for Testing and Materials.

ASTM (1981b). Standard test methods for tensile properties of thin plastic sheeting. D882-80a. Philadelphia: American Society for Testing and Materials.

Chanda, M., & Roy, S. K. (1998). *Plastics technology handbook* (3rd ed.). New York: Marcel Dekker.

Chang, Y. P., Cheah, P. B., & Seow, C. C. (2000). Plasticizing–antiplasticizing effects of water on physical properties of tapioca starch films in the glassy state. *Journal of Food Science, 65*(2), 1–7.

Chen, R. H., & Tsaih, M. L. (1998). Effect of temperature on the intrinsic viscosity and conformation of chitosan in dilute HCL solution. *International Journal of Biological Macromolecules, 23*, 135–141.

Chen, R. H., Tsaih, M. L., & Lin, W. C. (1996). Effects of chain flexibility of chitosan molecules on the preparation, physical, and release characteristics of the prepared capsule. *Carbohydrate Polymers, 31*, 141–148.

Cheng, L. H., Abd Karim, A., Norziah, M. H., & Seow, C. C. (2002). Modification of the microstructural and physical properties of konjac glucomannan-based films by alkali and sodium carboxymethylcellulose. *Food Research International, 35*, 829–836.

Cui, R., & Oates, C. G. (1999). The effect of amylose lipid complex formation on enzyme susceptibility of sago starch. *Food Chemistry, 65*, 417–425.

Gontard, N., Guilbert, S., & Cuq, J. L. (1993). Water and glycerol as plasticizers affect mechanical and water vapor barrier properties of an edible wheat gluten film. *Journal of Food Science, 58*, 206–211.

Greenspan, L. (1977). Humidity fixed points of binary saturated aqueous solutions. *Journal of Research of the National Bureau of Standards – A. Physics and Chemistry, 81*(1), 89–96.

Grosvenor, M. P., & Staniforth, J. N. (1996). The effect of molecular weight on the rheological and tensile properties of poly(ε-caprolactone). *International Journal of Pharmaceutics, 135*, 103–109.

Krishnarau, L., & Hoseney, R. C. (1994). Acid-hydrolyzed starch tailings effects on cookies spread. *Journal of Food Science, 59*, 1255–1257, 1270.

Kumar, V. N. G., Bhandari, M. V., & Bhat, A. N. (1991). Modifications of tapioca starch properties by polyethylene glycol (4000) and polyethylene glycol (4000) stearate additives. *Starch/Stärke, 43*(3), 93–98.

Kurata, M., & Tsunashima, Y. (1989). Viscosity–molecular weight relationships and unperturbed dimensions of linear chain molecules. In J. Brandrup & E. H. Immergut (Eds.), *Polymer handbook* (3rd ed.). New York: John Wiley & sons.

Nielsen, P. M. (1997). Functionality of protein hydrolysates. In A. P. Srinivasan Damodaran (Ed.), *Food proteins and their applications* (pp. 443–472). New York: Marcel Dekker Inc.

Ofori-Kwakye, K., & Fell, J. T. (2001). Biphasic drug release: the permeability of films containing pectin, chitosan and HPMC. *International Journal of Pharmaceutics, 226*, 139–145.

Rohwer, R. G., & Klem, R. E. (1984). Acid-modified starch: production and uses. In R. L. Whistler, J. N. BeMiller, & E. F. Paschall (Eds.), *Starch: chemistry and technology* (2nd ed., pp. 529–539). London: Academic Press.

Shamekh, S., Myllarinen, P., Poutanen, K., & Forssell, P. (2002). Film formation properties of potato starch hydrolysates. *Starch/Stärke, 54*, 20–24.

Sothornvit, R., & Krochta, J. M. (2000a). Oxygen permeability and mechanical properties of films from hydrolyzed whey protein. *Journal of Agricultural and Food Chemistry, 48*, 3913–3916.

Sothornvit, R., & Krochta, J. M. (2000b). Water vapor permeability and solubility of films from hydrolyzed whey protein. *Journal of Food Science, 65*, 700–703.

Spiess, W. E. L., & Wolf, W. R. (1983). The result of the Cost 90 project on water activity. In R. Jowitt, F. Escher, F. B. Hallstrom, M. E. Meffert, W. E. L. Spiess, & G. Vos (Eds.), *Physical properties of foods*. London: Applied Science Publisher.

Takigami, S. (2000). Konjac mannan. In G. O. Phillips & P. A. Williams (Eds.), *Handbook of hydrocolloids*. England: Woodhead Publishing Limited.

Takigami, S., Takiguchi, T., & Philips, G. O. (1997). Microscopical studies of the tissue structure of konjac tubers. *Food Hydrocolloids, 11*(4), 479–484.

Yoshimura, M., & Nishinari, K. (1999). Dynamic viscoelastic study on the gelation of konjac glucomannan with different molecular weights. *Food Hydrocolloids, 13*, 227–233.

Zhang, H., Yoshimura, M., Nishinari, K., Williams, M. A. K., Foster, T. J., & Norton, I. T. (2001). Gelation behavior of konjac glucomannan with different molecular weights. *Biopolymers, 59*, 38–50.